DALTON
FULL PAPER

Protonation reactions of the salts [Na][Pt(PR_3)$_2$(η^5-7-$CB_{10}H_{11}$)] (PR_3 = PEt_3 or PMe_2Ph): synthesis and crystal structures of the platinacarborane complexes [PtCl(PMe_2Ph)$_2$(η^5-7-$CB_{10}H_{11}$)], [Pt_2{μ-σ,η^5:σ′,$\eta^{5\prime}$-8,9′-(7-$CB_{10}H_{10}$)$_2$}(PMe_2Ph)$_4$] and [Pt_2(PEt_3)$_4${η^5:$\eta^{5\prime}$-9,9′-I(H)(7-$CB_{10}H_{10}$)$_2$}]†

Ian Blandford,[a] John C. Jeffery,[a] Helen Redfearn,[a] Leigh H. Rees,[a] Martin D. Rudd[b] and F. Gordon A. Stone*[,b]

[a] *School of Chemistry, The University, Bristol, UK BS8 1TS*
[b] *Department of Chemistry, Baylor University, Waco, TX 76798-7348, USA*

Protonation of [Na][Pt(PMe_2Ph)$_2$(η^5-7-$CB_{10}H_{11}$)] **1b** with HCl in diethyl ether afforded a mixture of the complexes [PtX(PMe_2Ph)$_2$(η^5-7-$CB_{10}H_{11}$)] (X = H **2b** or Cl **3**) and [Pt_2{μ-σ,η^5:σ′,$\eta^{5\prime}$-8,9′-(7-$CB_{10}H_{10}$)$_2$}(PMe_2Ph)$_4$] **4**. Single-crystal X-ray diffraction studies established the structures of **3** and **4**. In the former the platinum atom is co-ordinated on one side by the open CBBBB face of the *nido*-7-$CB_{10}H_{11}$ cage and on the other by a chlorine atom and two PMe_2Ph molecules. In the molecule **4** two *nido*-icosahedral CB_{10} cage frameworks, each η^5-co-ordinated by their open CBBBB faces to a platinum atom, are joined by a B–B connectivity and by two relatively long Pt–B connectivities. The B–B link is formed between a boron atom in a β site in one CB*B*BB ring and a boron in an α site in the other C*B*BBB ring. Each boron involved in this connectivity also forms a B–Pt linkage to the platinum atom in the adjacent *closo*-2,1-$PtCB_{10}$ sub-cluster. Thus the two metal atoms and the two borons form a 'butterfly' arrangement with the platinums at the wing-tips. Treatment of [Na][Pt(PEt_3)$_2$(η^5-7-$CB_{10}H_{11}$)] with HCl in diethyl ether gave [PtH(PEt_3)$_2$(η^5-7-$CB_{10}H_{11}$)] **2a** as expected, but a complex mixture of other products was also formed. Addition of [NEt_4]I to this mixture allowed isolation of a species [Pt_2(PEt_3)$_4${η^5:$\eta^{5\prime}$-9,9′-I(H)(7-$CB_{10}H_{10}$)$_2$}] **5**. This unusual formulation is based principally on the results of an X-ray diffraction study which revealed that two icosahedral *closo*-2,1-$PtCB_{10}$ sub-clusters were bridged by an iodine atom.

As part of a program to develop the neglected area of monocarbon metallacarbaboranes with icosahedral frameworks[2] we have recently prepared the reagent [Na][Pt(PEt_3)$_2$(η^5-7-$CB_{10}H_{11}$)] **1a** and described several reactions of this new species, including its protonation with HBF_4·Et_2O to give [PtH(PEt_3)$_2$(η^5-7-$CB_{10}H_{11}$)] **2a**.[1] Extending these studies we have synthesized the related salt [Na][Pt(PMe_2Ph)$_2$(η^5-7-$CB_{10}H_{11}$)] **1b**. Herein we report the protonation of this compound with HCl, a reaction which affords a mixture of products including a diplatinum species in which two $PtCB_{10}$ sub-clusters are conjoined by a B–B bond and two Pt–B connectivities. A diplatinum complex with a very unusual structure was also isolated when **1a** was similarly protonated with HCl followed by addition of [NEt_4]I.

Results and Discussion

A solution of compound **1b** in thf (tetrahydrofuran) was prepared *in situ* from the reagents [Na]$_3$[*nido*-7-$CB_{10}H_{11}$] and [$PtCl_2(PMe_2Ph)_2$]. A diethyl ether solution of HCl was then added to the mixture formed. Column chromatography separated three reaction products: two mononuclear platinum species [PtX(PMe_2Ph)$_2$(η^5-7-$CB_{10}H_{11}$)] (X = H **2b** or Cl **3**), and a diplatinum complex [Pt_2{μ-σ,η^5:σ′,$\eta^{5\prime}$-8,9′-(7-$CB_{10}H_{10}$)$_2$}(PMe_2Ph)$_4$] **4**. Compounds **2b** and **4** were each formed in about equal amounts (*ca.* 15–20% based on the platinum used) while **3** was produced in lesser amount (*ca.* 10%). The formation of **2b** was expected and co-formation of **3** can readily be understood as occurring *via* reaction of the hydrido complex with the HCl. Both complexes were fully characterised by microanalysis and NMR data (Table 1). As discussed below, the nature of **3** was further established by an X-ray diffraction study.

The ^{1}H NMR spectrum of compound **2b** shows a triplet resonance at δ −8.27 [J(PH) = 29, J(PtH) = 1074 Hz] diagnostic for the PtH group, and a broad peak at δ 2.66 characteristic for the cage CH proton. The corresponding signals in the ^{1}H spectrum of **2a** are seen at δ −8.78 [J(PH) = 27, J(PtH) = 1030 Hz] and 2.41, respectively.[1] Other signals in the ^{1}H NMR spectrum of **2b** are as expected. The ^{31}P-{^{1}H} NMR spectrum shows a singlet resonance at δ −15.2 with ^{195}Pt satellite peaks [J(PtP) = 1859 Hz], and the ^{11}B-{^{1}H} NMR spectrum displayed five broad peaks of relative intensity 1:4:1:2:2, both spectra being of similar pattern to those of **2a**.

The NMR data for compound **3** (Table 1) call for no special comment. Selected bond distances and angles from the X-ray diffraction study are listed in Table 2 and the molecule is shown in Fig. 1. On one side the platinum atom is ligated in the usual pentahapto manner by the open CBBBB face of the carbaborane cage [Pt(1)–C(1) 2.240(2), Pt(1)–B(2) 2.231(3), Pt(1)–B(3) 2.264(3), Pt(1)–B(4) 2.226(3), Pt(1)–B(5) 2.232(3) Å], and on the other by the phosphine ligands [Pt(1)–P(1) 2.4162(6), Pt(1)–P(2) 2.3399(6) Å] and the halogen atom [Pt(1)–Cl 2.4469(6) Å]. These bond distances are comparable with those previously observed in complexes containing a $PtCl(PMe_2Ph)_2$ moiety.[3]

The nature of the third product **4** of the reaction only became apparent after an X-ray diffraction study had been

† The complexes described have a platinum atom incorporated into a *closo*-1-carba-2-platinadodecaborane structure. However, to avoid a complicated nomenclature, and to relate the compounds to species with pentahapto co-ordinated cyclopentadienyl ligands, following precedent (see ref. 1) we treat the cages as *nido*-11-vertex ligands with numbering as for an icosahedron from which the twelfth vertex has been removed.

Table 1 Proton, ^{13}C, ^{11}B and ^{31}P NMR data for the new complexes[a]

Compound	^{1}H (δ)	^{13}C (δ)[b]	^{11}B (δ)[c]	^{31}P (δ)[d]
2b	−8.27 [t, 1 H, PtH, *J*(PH) 29, *J*(PtH) 1074], 1.80 (m, 12 H, Me), 2.66 (s br, 1 H, cage CH), 7.44–7.46 (m, 10 H, Ph)	136.1–129.4 (Ph),[e] 13.1 (m, Me)	12.1 (1 B), −3.8 (4 B), −6.6 (1 B), −12.9 (2 B), −17.0 (2 B)	−15.2 [s, *J*(PtP) 1859]
3	1.80 [d, 6 H, Me, *J*(PH) 8], 1.92 [d, 6 H, Me, *J*(PH) 8], 3.50 (s br, 1 H, cage CH), 7.45–7.69 (m, 10 H, Ph)	138.9–130.1 (Ph), 58.6 (br, cage CH), 14.0–13.0 (m, Me)	19.2 (1 B), 5.1 (br, 3 B), −5.6 (2 B), −8.6 (2 B), −14.0 (2 B)	−4.4 [s, *J*(PtP) 2325]
4	1.77–2.15 (m, 24 H, Me), 2.64 (br, 2 H, cage CH), 6.89–8.05 (m, 20 H, Ph)	136.9–128.6 (Ph), 49.1 (vbr, cage CH), 14.7–13.7 (m, Me)	12.6 (2 B), 4.1 (1 B), 2.3 (2 B), −1.3 (2 B), −5.0 (1 B), −7.8 (2 B), −9.9 (4 B), −13.8 (2 B), −17.1 (4 B)	−8.5 [d, *J*(PP) 32, *J*(PtP) 2668], −13.8 [d, *J*(PP) 36, *J*(PtP) 3713], −21.4 [d, *J*(PP) 36, *J*(PtP) 3268], −25.4 [d, *J*(PP) 32, *J*(PtP) 3034]
5	1.03–1.20 (m, 36 H, Me), 2.03–2.27 (m, 24 H, CH_2), 2.92 (br s, 2 H, cage CH)	—	11.6 (2 B), 4.5 (4 B), −4.7 (4 B), −8.8 (4 B), −12.0 (4 B), −16.4 (2 B)	−2.1 [d, *J*(PP) 29, *J*(PtP) 2816], −7.9 [d, *J*(PP) 29, *J*(PtP) 2796] and −2.5 [d, *J*(PP) 29, *J*(PtP) 3300], −8.9 [d, *J*(PP) 29, *J*(PtP) 2661]

[a] Chemical shifts (δ) in ppm, coupling constants (*J*) in Hz, measurements in CD_2Cl_2 at room temperature. [b] Hydrogen-1 decoupled, chemical shifts are positive to high frequency of $SiMe_4$. [c] Hydrogen-1 decoupled, chemical shifts are positive to high frequency of $BF_3{\cdot}Et_2O$ (external). [d] Hydrogen-1 decoupled, chemical shifts are positive to high frequency of 85% H_3PO_4 (external). [e] Cage-carbon resonance not seen due to weak spectrum.

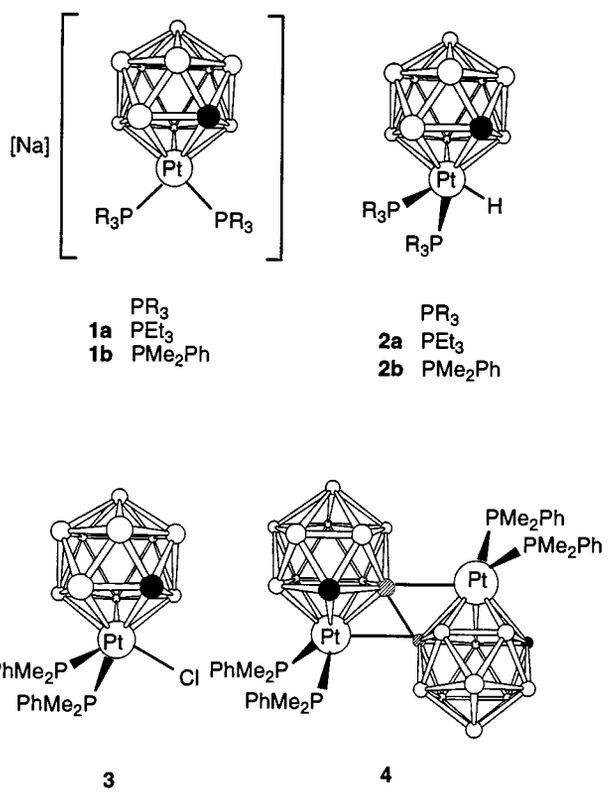

carried out on a single crystal. The molecule $[Pt_2\{\mu\text{-}\sigma,\eta^5\text{:}\sigma',\eta^{5'}\text{-}8,9'\text{-}(7\text{-}CB_{10}H_{10})_2\}(PMe_2Ph)_4]$ is shown in Fig. 2 and selected interatomic connectivities and angles are listed in Table 3. There are two *nido*-7-CB_{10} cage frameworks joined by a B–B connectivity [B(14)–B(22) 1.726(8) Å] and by two relatively long Pt–B connectivities [Pt(1)–B(22) 2.660(6), Pt(2)–B(14) 2.632(6) Å]. The open CBBBB face of each cage is co-ordinated to a platinum atom in the η^5 manner, with Pt–C (average 2.292 Å) and Pt–B (average 2.255 Å) distances comparable with those in **2a**[1] and **3**. A noteworthy feature of the structure, which we believe has no precedent in monocarbon metallacarbaborane chemistry, are the sites occupied by the boron atoms B(14) and B(22) in their respective CBBBB rings. Atom B(14) is in a β site in the CB*B*BB ring pentahapto co-ordinated to Pt(1) whereas B(22) is in an α site in the C*B*BBB ring co-ordinated to Pt(2). The atoms

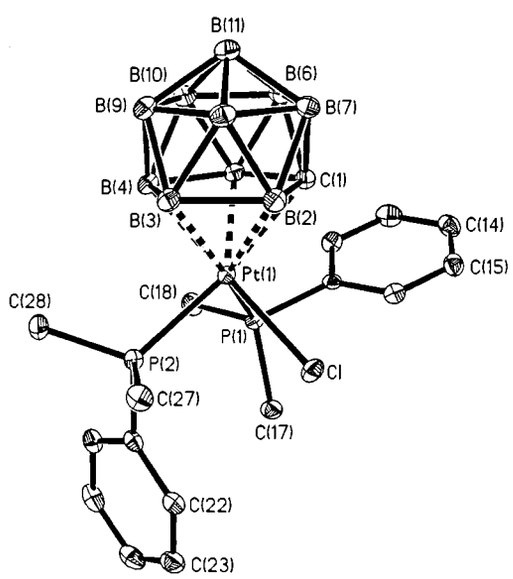

Fig. 1 Molecular structure of $[PtCl(PMe_2Ph)_2(\eta^5\text{-}7\text{-}CB_{10}H_{11})]$ **3** showing the atom labelling scheme. Ellipsoids are drawn at the 40% probability level and hydrogen atoms are omitted for clarity

Pt(1)B(14)Pt(2)B(22) form a 'butterfly' framework with the two metal atoms at the wing-tips and with B(14)–B(22) forming the body. The atoms of the 'butterfly' framework are almost coplanar, the dihedral angle between the planes defined by Pt(1)B(14)B(22) and Pt(2)B(14)B(22) being *ca.* 168°.

The Pt(1)B(14)Pt(2)B(22) arrangement in compound **4** is similar to that of four boron atoms which join together two *nido*-7,8-$C_2B_9H_{11}$ cage systems in the macropolyhedral carbaborane $C_4B_{18}H_{22}$.[4] In this molecule there are three B–B connectivities linking the two *nido*-7,8-C_2B_9 sub-clusters whereas in **4** there is one B–B and two Pt–B connectivities joining the two *closo*-2,1-$PtCB_{10}$ halves of the molecule. In $C_4B_{18}H_{22}$ the B–B distance [1.652(2) Å] comprising the body of the 'butterfly' is the shortest B–B separation, and this separation is also somewhat shorter than the corresponding connectivity in **4** [B(14)–B(22) 1.726(8) Å]. It has been suggested[4] that the intercluster linkage between the two *nido*-7,8-C_2B_9 fragments in $C_4B_{18}H_{22}$ can be accounted for in terms of two three-centre two-electron bonds between the four boron atoms joining the C_2B_9 units. A similar description can be given for the bonding in the

Table 2 Selected internuclear distances (Å) and angles (°) for $[PtCl(PMe_2Ph)_2(\eta^5\text{-}7\text{-}CB_{10}H_{11})]$ **3** with estimated standard deviations (e.s.d.s) in parentheses

Pt(1)–B(4)	2.226(3)	Pt(1)–B(2)	2.231(3)	Pt(1)–B(5)	2.232(3)	Pt(1)–C(1)	2.240(2)
Pt(1)–B(3)	2.264(3)	Pt(1)–P(2)	2.3399(6)	Pt(1)–P(1)	2.4162(6)	Pt(1)–Cl	2.4469(6)
C(1)–B(6)	1.698(4)	C(1)–B(7)	1.704(4)	C(1)–B(5)	1.732(4)	C(1)–B(2)	1.769(4)
B(2)–B(8)	1.764(4)	B(2)–B(7)	1.779(4)	B(2)–B(3)	1.829(4)	B(3)–B(9)	1.768(4)
B(3)–B(8)	1.776(4)	B(3)–B(4)	1.869(4)	B(4)–B(9)	1.785(4)	B(4)–B(10)	1.794(4)
B(4)–B(5)	1.854(4)	B(5)–B(10)	1.752(4)	B(5)–B(6)	1.781(4)	B(6)–B(7)	1.766(4)
B(6)–B(11)	1.773(4)	B(6)–B(10)	1.774(4)	B(7)–B(8)	1.769(4)	B(7)–B(11)	1.776(4)
B(8)–B(9)	1.780(4)	B(8)–B(11)	1.781(4)	B(9)–B(11)	1.775(4)	B(9)–B(10)	1.786(4)
B(10)–B(11)	1.778(4)	P(7)–C(18)	1.808(2)	P(1)–C(17)	1.817(2)	P(1)–C(11)	1.821(2)
P(2)–C(28)	1.812(2)	P(2)–C(27)	1.814(2)	P(2)–C(21)	1.816(2)		
C(1)–Pt(1)–P(2)	162.39(6)	C(1)–Pt(1)–P(1)	98.84(6)	C(1)–Pt(1)–Cl	98.47(6)	P(2)–Pt(1)–Cl	84.33(2)
P(1)–Pt(1)–Cl	83.88(2)	C(18)–P(1)–C(17)	102.57(12)	C(18)–P(1)–C(11)	106.90(11)	C(17)–P(1)–C(11)	101.9(1)
C(18)–P(1)–Pt(1)	115.12(9)	C(17)–P(1)–Pt(1)	120.0(8)	C(11)–P(1)–Pt(1)	108.91(7)	C(28)–P(2)–C(27)	104.8(1)
C(28)–P(2)–C(21)	103.19(11)	C(27)–P(2)–C(21)	103.69(11)	C(28)–P(2)–Pt(1)	116.03(9)	C(27)–P(2)–Pt(1)	111.38(9)
C(21)–P(2)–Pt(1)	116.40(7)						

Table 3 Selected internuclear distances (Å) and angles (°) for $[Pt_2(\mu\text{-}\sigma,\eta^5\!:\!\sigma',\eta^{5\prime}\text{-}8,9'\text{-}(7\text{-}CB_{10}H_{10})_2\}(PMe_2Ph)_4]$ **4** with e.s.d.s in parentheses

Pt(1)–B(13)	2.237(6)	Pt(1)–B(15)	2.243(6)	Pt(1)–B(12)	2.269(6)	Pt(1)–B(14)	2.275(6)
Pt(1)–P(1)	2.3343(14)	Pt(1)–P(2)	2.342(2)	Pt(1)–C(11)	2.380(5)	Pt(1)–B(22)	2.660(6)
P(1)–C(38)	1.813(6)	P(1)–C(31)	1.827(6)	P(1)–C(37)	1.834(5)	P(2)–C(47)	1.808(6)
P(2)–C(48)	1.812(6)	P(2)–C(41)	1.821(6)	Pt(2)–C(21)	2.204(5)	Pt(2)–B(23)	2.236(6)
Pt(2)–B(25)	2.243(6)	Pt(2)–B(22)	2.246(6)	Pt(2)–B(24)	2.290(5)	Pt(2)–P(4)	2.3201(14)
Pt(2)–P(3)	2.3674(14)	P(3)–C(51)	1.821(6)	P(3)–C(57)	1.823(5)	P(3)–C(58)	1.826(5)
P(4)–C(68)	1.813(6)	P(4)–C(67)	1.818(5)	P(4)–C(61)	1.826(5)	Pt(2)–B(14)	2.632(6)
B(14)–B(22)	1.726(8)						
P(1)–Pt(1)–P(2)	95.43(5)	P(1)–Pt(1)–C(11)	126.47(13)	P(2)–Pt(1)–C(11)	97.78(14)	P(1)–Pt(1)–B(22)	108.1(1)
Pt(2)–Pt(1)–B(22)	103.66(13)	C(11)–Pt(1)–B(22)	118.5(2)	Pt(1)–B(14)–Pt(2)	138.0(3)	P(4)–Pt(2)–P(3)	94.66(5)
Pt(2)–B(22)–Pt(1)	138.1(3)	P(3)–Pt(2)–B(14)	105.41(13)	P(1)–Pt(2)–B(14)	105.7(2)	C(21)–Pt(2)–P(4)	171.0(1)
C(21)–Pt(2)–P(3)	94.33(14)						

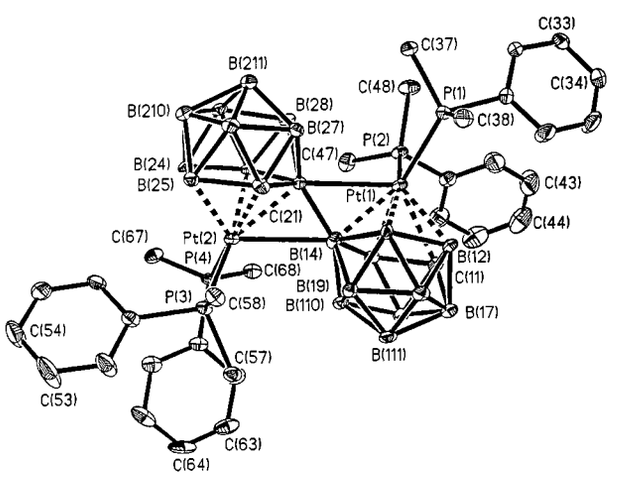

Fig. 2 Molecular structure of $[Pt_2\{\mu\text{-}\sigma,\eta^5\!:\!\sigma',\eta^{5\prime}\text{-}8,9'\text{-}(7\text{-}CB_{10}H_{10})_2\}(PMe_2Ph)_4]$ **4**. Details as in Fig. 1

Pt(1)B(14)Pt(2)B(22) unit of **4**. Moreover, it is noteworthy that the $Pt(PMe_2Ph)_2$ moieties in **4** are isolobal with the BH fragments which occupy the wing-tip positions in the central B_4 'butterfly' of $C_4B_{18}H_{22}$.

The Pt–P distances in compound **4** (average 2.341 Å) are as expected [3] and the phosphorus atoms are disposed quite symmetrically above and below the Pt(1)B(14)Pt(2)B(22) 'butterfly' framework. Whilst the CBBBB faces of the cages are somewhat twisted away from one another, as they seem to be also in $C_4B_{18}H_{22}$, distortions of this type would not be important in solution. It is therefore important to note that it is the presence of the atoms B(14) and B(22) which adopt asymmetric β and α positions with respect to their cage CH atoms which precludes the possibility of complex **4** achieving high symmetry in solution. Thus all four phosphorus atoms and all twenty boron atoms in the complex are formally chemically inequivalent, a feature which is consistent with the spectroscopic data (Table 1) reported below.

The pathway by which compound **4** is produced by treating **1b** with HCl is not at present known but appears to involve oxidation of the complex anion in **1b**, followed by a combination of two $Pt(PMe_2Ph)_2(\eta^5\text{-}7\text{-}CB_{10}H_{11})$ groups with loss of molecular hydrogen. Interestingly, $C_4B_{18}H_{22}$ is formed [4] by loss of hydrogen upon oxidation of the anion $[nido\text{-}7,8\text{-}C_2B_9H_{12}]^-$. Unfortunately detailed NMR studies on **4** could not be made due to its poor solubility and its formation in small amounts. However, the ^1H and $^{13}C\text{-}\{^1H\}$ NMR spectra (Table 1) revealed broad diagnostic resonances for the two inequivalent cage CH groups at δ 2.64 and 49.1, respectively, which were unfortunately unresolved. Similarly the $^{11}B\text{-}\{^1H\}$ NMR spectrum showed only very broad peaks as expected for a complex which in principle should show 20 inequivalent resonances. The $^{31}P\text{-}\{^1H\}$ NMR spectrum displayed four doublet resonances for the four chemically inequivalent PMe_2Ph ligands consistent with the structure revealed by the X-ray diffraction study.

The results of protonating compound **1b** with HCl prompted an examination of a similar protonation of **1a** with this acid. This reaction afforded a mixture of several products some of which formed in only trace amounts and could not be identified. The hydrido complex **2a** was the expected product and this compound was indeed formed but in low yield (*ca.* 10–15%). It could be separated from the other products by column chromatography. There was no evidence for formation of a chloro analogue of **3**. A $^{11}B\text{-}\{^1H\}$ NMR examination of the crude mixture revealed the presence of the salt $[Na][nido\text{-}7\text{-}CB_{10}H_{13}]$ leading to the suspicion that other salt-like products might also be present. Accordingly $[NEt_4]I$ was added in an attempt to facilitate isolation of any anionic platinum complexes as their $[NEt_4]^+$ salts. Following work-up, a green crystalline compound was obtained (*ca.* 10% yield) the mass spectrum of which revealed a molecular ion at *m/z* 1251 and peaks corresponding

Table 4 Selected internuclear distances (Å) and angles (°) for $[Pt_2(PEt_3)_4\{\eta^5:\eta^{5'}\text{-}9,9'\text{-}I(H)(7\text{-}CB_{10}H_{10})_2\}]$ **5** with e.s.d.s in parentheses

Pt(2)–B(25)	2.251(6)	Pt(2)–B(22)	2.257(6)	Pt(2)–B(21)	2.262(6)	Pt(2)–P(4)	2.306(2)
Pt(2)–B(23)	2.316(6)	Pt(2)–P(3)	2.335(2)	Pt(2)–C(24)	2.435(6)	Pt(1)–B(12)	2.226(6)
Pt(1)–B(11)	2.240(6)	Pt(1)–B(13)	2.253(7)	Pt(1)–B(15)	2.260(6)	Pt(1)–P(1)	2.357(2)
Pt(1)–P(2)	2.3691(14)	Pt(1)–C(14)	2.392(6)	Pt(1)···I	2.8749(8)	I–B(11)	2.167(7)
I–B(21)	2.197(6)	I–H(1)	0.8570(4)	P(1)–C(33)	1.824(7)	P(1)–C(31)	1.826(7)
P(1)–C(35)	1.838(7)	P(2)–C(41)	1.808(6)	P(2)–C(43)	1.832(6)	P(2)–C(45)	1.838(6)
C(41)–C(42)	1.535(8)	P(3)–C(51)	1.830(6)	P(3)–C(53)	1.842(6)	P(3)–C(55)	1.846(6)
P(4)–C(63)	1.826(6)	P(4)–C(61)	1.826(6)	P(4)–C(65)	1.846(6)		
B(25)–Pt(2)–B(22)	80.5(2)	B(25)–Pt(2)–B(21)	48.1(2)	B(22)–Pt(2)–B(21)	46.6(2)	B(25)–Pt(2)–P(4)	169.2(2)
B(22)–Pt(2)–P(4)	95.0(2)	B(21)–Pt(2)–P(4)	133.7(2)	B(25)–Pt(2)–B(23)	75.1(2)	B(22)–Pt(2)–B(23)	47.3(2)
B(21)–Pt(2)–B(23)	77.5(2)	P(4)–Pt(2)–B(23)	94.6(2)	B(25)–Pt(2)–P(3)	87.4(2)	B(22)–Pt(2)–P(3)	164.5(2)
B(21)–Pt(2)–P(3)	117.9(2)	P(4)–Pt(2)–P(3)	98.48(5)	B(23)–Pt(2)–P(3)	138.2(2)	B(25)–Pt(2)–C(24)	43.7(2)
B(22)–Pt(2)–C(24)	76.0(2)	B(21)–Pt(2)–C(24)	75.9(2)	P(4)–Pt(2)–C(24)	125.7(2)	B(23)–Pt(2)–C(24)	40.9(2)
P(3)–Pt(2)–C(24)	101.9(2)	B(12)–Pt(1)–B(11)	47.5(2)	B(12)–Pt(1)–B(13)	48.5(2)	B(11)–Pt(1)–B(13)	80.5(3)
B(12)–Pt(1)–B(15)	81.4(3)	B(11)–Pt(1)–B(15)	48.9(2)	B(13)–Pt(1)–B(15)	77.2(3)	B(12)–Pt(1)–P(1)	173.5(2)
B(11)–Pt(1)–P(1)	126.1(2)	B(13)–Pt(1)–P(1)	133.4(2)	B(15)–Pt(1)–P(1)	92.9(2)	B(12)–Pt(1)–P(2)	91.3(2)
B(11)–Pt(1)–P(2)	129.9(2)	B(13)–Pt(1)–P(2)	91.8(2)	B(15)–Pt(1)–P(2)	169.0(2)	P(1)–Pt(1)–P(2)	94.78(5)
B(12)–Pt(1)–C(14)	78.0(2)	B(11)–Pt(1)–C(14)	77.7(2)	B(13)–Pt(1)–C(14)	43.4(2)	B(15)–Pt(1)–C(14)	43.4(2)
P(1)–Pt(1)–C(14)	100.0(2)	P(2)–Pt(1)–C(14)	127.1(2)	B(12)–Pt(1)–I	81.9(2)	B(11)–Pt(1)–I	48.2(2)
B(13)–Pt(1)–I	126.9(2)	B(15)–Pt(1)–I	77.7(2)	P(1)–Pt(1)–I	93.88(5)	P(2)–Pt(1)–I	109.48(4)
C(14)–Pt(1)–I	119.6(2)	B(11)–I–B(21)	112.1(3)	B(11)–I–Pt(1)	50.4(2)	B(21)–I–Pt(1)	119.3(2)
B(11)–I–H(1)	159.0(2)	B(21)–I–H(1)	87.6(2)	Pt(1)–I–H(1)	126.76(3)		

to the sequential loss of two PEt_3 ligands and an iodine atom. The NMR data indicated the presence of two $Pt(PEt_3)_2$ groups and two cage systems. This product is formulated as $[Pt_2(PEt_3)_4\{\eta^5:\eta^{5'}\text{-}9,9'\text{-}I(H)(7\text{-}CB_{10}H_{10})_2\}]$ **5** on the basis of an X-ray diffraction study and considerations based on skeletal electron-pair theory. The structure is shown in Fig. 3 and significant internuclear distances and angles are listed in Table 4.

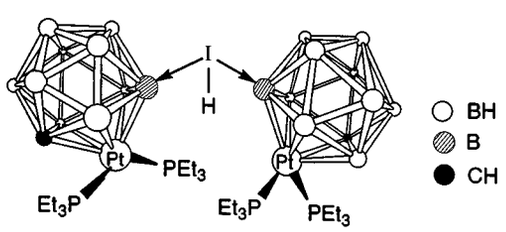

5

The molecule has two $Pt(PEt_3)_2(\eta^5\text{-}7\text{-}CB_{10}H_{10})$ units bridged by an iodine atom [B(11)–I 2.167(7), B(21)–I 2.197(6) Å, B(11)–I–B(21) 112.1(3)°]. Thus formally compound **5** results from replacement of a cage H atom in each of two anions of **1a** by iodine. Moreover, in both halves of the molecule the boron atoms linked to the iodine are in a β site with respect to the carbons in the CB*B*BB rings ligating the Pt atoms. The average Pt–P distance in **5** (2.342 Å) is as expected being only slightly longer than that found in $[Pt(CO)(PPh_3)(\eta^5\text{-}7\text{-}CB_{10}H_{11})]^-$ [2.3093(1) Å].[1]

There is a weak interaction between Pt(1) and the bridging I atom [Pt(1)···I 2.8749(8) Å] but if this is ignored the complex has an approximate non-crystallographic two-fold axis of symmetry which is coincident with the bisector of the B(11)–I–B(21) angle. Compound **5** thus has two almost chemically equivalent pairs of phosphorus atoms [P(1), P(3) and P(2), P(4)] a feature discussed below in more detail with the spectroscopic data. The presence of two carbaborane cages joined by a bridging halide is not entirely without precedent. Thus in the compound $[9,9'\text{-}Br\text{-}(1,7\text{-}C_2B_{10}H_{11})_2][BF_4]$[5] two *closo*-$C_2B_{10}H_{11}$ cages are linked by a bridging Br ligand. Moreover, the average B–Br–B angle for the two crystallographically independent molecules found in the solid-state structure is 111.7°, which is remarkably similar to the B(11)–I–B(21) angle [112.1(3)°] observed in **5**.

The attachment of an H atom to the iodine in compound **5** allows a satisfactory explanation for the valence electron count in this cluster which would not be possible if it were absent. Although, the quality of the structure determination of **5** did not allow unambiguous location of this proton, a weak residual peak [H(1)] was found in the final difference density map. The coordinates of H(1) could not be refined and its location, whilst chemically reasonable, should be treated with appropriate caution. The HI group *via* its iodine atom can be regarded as formally donating an electron pair to each *closo*-2,1-$PtCB_{10}H_{10}$ fragment. In this manner the icosahedral $PtCB_{10}H_{10}I$ moieties attain the necessary 13 skeletal electron pairs for a filled orbital description, it being noted that a $Pt(PEt_3)_2$ metal–ligand group contributes two electrons for cluster bonding like a BH vertex, and an I→B vertex would contribute three electrons behaving like a CH unit. Each half of the molecule in **5** is thus similar to $C_2B_{10}H_{12}$ for electron-counting purposes. The previously noted weak Pt(1)···I [2.8749(8) Å] interaction may provide a route by which charge may be returned from Pt to the iodine centre thereby enhancing its ability to serve as a Lewis-base donor to the two-electron deficient Lewis-acidic boron cages. The

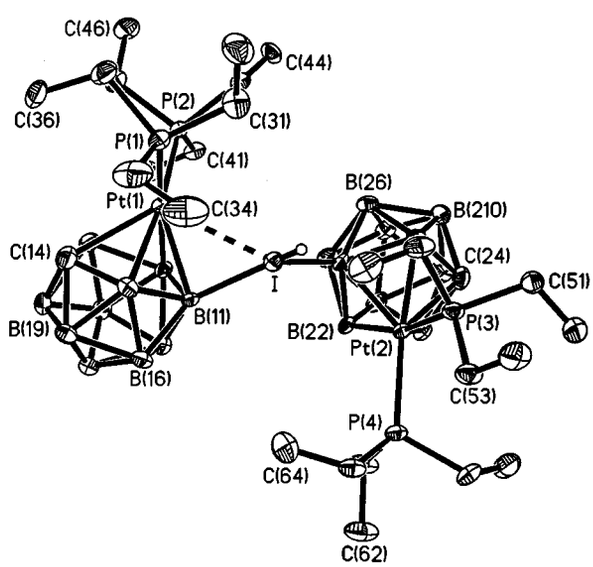

Fig. 3 Molecular structure of $[Pt_2(PEt_3)_4\{\eta^5:\eta^{5'}\text{-}9,9'\text{-}I(H)(7\text{-}CB_{10}H_{10})_2\}]$ **5** showing the atom labelling scheme. Ellipsoids are drawn at the 40% probability level and except for H(I) hydrogen atoms are omitted for clarity

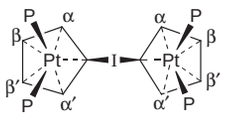

Diastereoisomer	Predicted no. of ^{31}P NMR resonances
ββ	2
ββ'	2
αβ or α′β′	4
α′β or αβ′	4
αα	2
αα'	2

Fig. 4 The possible diastereoisomers for complex **5**. Only the metal ligating atoms of the carbaborane cage are shown

relatively long Pt(2)···I separation (3.328 Å) indicates that the second platinum centre is not involved in enhancing the donor characteristics of the I atom in the solid state. However, in solution an exchange between Pt(1)–I and Pt(2)–I bonding might occur. Unfortunately well resolved ^{1}H NMR spectra of **5** free of impurities could not be obtained.

It is interesting to compare the role played by the bridging iodine in compound **5** with that of the bridging Br atom in [9,9′-Br-(1,7-$C_2B_{10}H_{11})_2$][BF_4].[5] In the latter compound the Br atom formally carries a positive charge and does not have an attached proton. The bromine cation contributes one electron to each $C_2B_{10}H_{11}$ fragment, effectively fulfilling the role of an exopolyhedral hydrogen for the borons to which the Br^+ is attached. In this manner the *closo*-$C_2B_{10}H_{11}$ moieties attain the necessary 13 skeletal electron pairs for a filled orbital description.

The similarity of the B–Br–B and B(11)–I–B(21) angles in [9,9′-Br-(1,7-$C_2B_{10}H_{11})_2$][BF_4] and compound **5** may be readily appreciated from a simple VSEPR analysis for the bridging halogens. In the former cluster the Br^+ ion has six electrons and receives a further two electrons from the ligated B atoms. There are thus four electron pairs at the Br, the geometry of which is therefore based upon a tetrahedron with two ligated B atoms and two lone pairs. The observed B–Br–B angle (111.7°) is very slightly greater than an ideal tetrahedral angle presumably reflecting the steric bulk of the two ligated cages. In compound **5** the neutral iodine atom has seven electrons plus one more from the attached H atom. In this cluster the boron atoms of the cages forming B–I bonds behave as Lewis acids accepting electron pairs from the iodine atom. The boron atoms therefore do not contribute to the electron count at the bridging iodine atom. Hence, the iodine atom in **5** also has four pairs of electrons and its geometry is thus also based upon a tetrahedral configuration associated with attachment to two boron atoms, one hydrogen atom and the presence of one lone pair. Again the observed B(11)–I–B(21) angle [112.1(3)°] is as expected for this geometry being very slightly greater than that found in [9,9′-Br-(1,7-$C_2B_{10}H_{11})_2$][BF_4], a feature which may well reflect the increased steric bulk of the Pt(PEt_3)$_2$-substituted carbaborane cages.

It was immediately apparent from examination of the ^{31}P-{^{1}H} NMR spectra of analytically pure crystalline samples of compound **5** that it must exist as more than one isomer in solution. These isomers almost certainly arise because the carbon atoms in the ligated faces of the carbaborane cages may occupy sites which are either α or β to the boron atom attached to iodine. The possible diastereoisomers together with the predicted number of ^{31}P-{^{1}H} NMR resonances are shown in Fig. 4. Using this nomenclature the isomer observed in the solid-state structure of **5** is ββ′ and there is no obvious reason why the closely related ββ isomer should not also be present in the reaction mixture. Both these isomers would be expected to show a pair of doublets with ^{195}Pt satellites in their ^{31}P-{^{1}H} NMR spectra and we therefore very tentatively assign the four strongest doublets observed in the ^{31}P-{H} NMR spectrum, and listed in Table 1, to these isomers. The remainder of the spectrum shows at least eight further weaker doublets which overlap both with each other and with poorly resolved ^{195}Pt satellites. These signals may be attributable to additional αβ and/or αα isomers present in the complex reaction mixture. The ^{31}P-{^{1}H} NMR spectrum remained unchanged at low temperature indicating that the isomers present are not undergoing exchange on the NMR timescale. Not surprisingly the ^{1}H and ^{11}B NMR spectra were relatively uninformative showing broad overlapping resonances in the expected regions.

Experimental

General

All experiments were conducted under an atmosphere of dry argon using Schlenk-tube techniques. Solvents were freshly distilled under nitrogen from appropriate drying agents before use. Light petroleum refers to that fraction of boiling point 40–60 °C. Tetrahydrofuran was distilled from potassium–benzophenone under nitrogen and stored over Na/K alloy. Flash chromatography columns (*ca*. 30 cm long and 3 cm in diameter) were packed under nitrogen with silica gel (Acros, 70–230 mesh). The NMR measurements were recorded at the following frequencies: ^{1}H at 360.13, ^{13}C at 90.56, ^{11}B at 115.55 and ^{31}P at 145.78 MHz. The reagents *nido*-7-NMe_3-7-$CB_{10}H_{12}$,[6] [$PtCl_2$(PEt_3)$_2$] and [$PtCl_2$(PMe_2Ph)$_2$][7] were prepared according to the literature methods, and [Na]$_3$[*nido*-$CB_{10}H_{11}$] was synthesized according to the procedure of Knoth *et al.*[8] The salts [Na][Pt(PEt_3)$_2$(η^5-7-$CB_{10}H_{11}$)] and [Na][Pt(PMe_2Ph)$_2$(η^5-7-$CB_{10}H_{11}$)] were prepared by the method described earlier.[1] A solution of HCl (1 mol dm^{-3}) in Et_2O (Aldrich) was used as supplied.

Preparations

Reaction of [Na][Pt(PMe_2Ph)$_2$(η^5-7-$CB_{10}H_{11}$)] with HCl. Orange-brown [Na][Pt(PMe_2Ph)$_2$(η^5-7-$CB_{10}H_{11}$)] was prepared *in situ* from [Na]$_3$[*nido*-$CB_{10}H_{11}$] (0.191 g, 1.00 mmol) and [$PtCl_2$(PMe_2Ph)$_2$] (0.542 g, 1 mmol) in thf (20 cm^3), and cooled to −96 °C. A solution of HCl in diethyl ether (1 cm^3) was then added. The mixture was warmed to room temperature over a period of 1 h and then stirred at 40 °C overnight producing a cloudy dark brown-green solution. Solvent was removed *in vacuo* and the residue was dissolved in CH_2Cl_2 (20 cm^3) and filtered through a Whatman 1 μm pore size Paradisc PTFE membrane to give a clear, dark yellow-green solution. The latter was concentrated to *ca.* 3 cm^3 and placed on the top of a silica gel column. Elution with CH_2Cl_2–light petroleum (1:1) removed a very pale yellow fraction followed by a dark purple band. Removal of the solvent from the light yellow band followed by crystallisation from CH_2Cl_2–Et_2O (1:8, 5 cm^3) yielded off-white *microcrystals* of [PtH(PMe_2Ph)$_2$(η^5-7-$CB_{10}H_{11}$)] **2b** (0.08 g, 15%) (Found: C, 33.5; H, 5.7. $C_{17}H_{34}B_{10}P_2Pt$ requires C, 33.8; H, 5.7%).

Further chromatographic elution of the dark purple band with the light petroleum–CH_2Cl_2 mixture yielded two closely eluting bands: a second yellow fraction followed by a dark purple fraction. Recrystallisation of the solids obtained by evaporation of both eluates was accomplished by layering concentrated CH_2Cl_2 solutions of each with hexane to afford yellow block-like *crystals* of [PtCl(PMe_2Ph)$_2$(η^5-7-$CB_{10}H_{11}$)] **3** (0.07 g, 10%) (Found: C, 32.4; H, 5.4. $C_{17}H_{33}B_{10}ClP_2Pt$ requires C, 32.0; H, 5.2%), and small purple cube-like *crystals* of [Pt_2{μ-σ,η^5:σ′,$\eta^{5\prime}$-8,9′-(7-$CB_{10}H_{10})_2$}(PMe_2Ph)$_4$] **4** (0.08 g, 20%) (Found: C, 33.1; H, 5.3. $C_{17}H_{32}B_{10}P_2Pt$ requires C, 33.9; H, 5.4%).

[Pt_2(PEt_3)$_4${η^5,$\eta^{5\prime}$-9,9′-I(H)(7-$CB_{10}H_{10})_2$}]. A cooled (−96 °C) thf (25 cm^3) solution of [Na][Pt(PEt_3)$_2$(η^5-7-$CB_{10}H_{11}$)] (0.56 g, 1 mmol) was treated with HCl in Et_2O (1 cm^3). In addition to the isolation of [PtH(PEt_3)$_2$(η^5-7-$CB_{10}H_{11}$)] **2a** (0.070 g, 13%)[1] by column chromatography after elution with CH_2Cl_2–light

Table 5 Crystallographic data and refinement details for compounds **3**–**5**

	3	**4**	**5**
Formula	$C_{17}H_{33}B_{10}ClP_2Pt$	$C_{34}H_{64}B_{20}P_4Pt_2 \cdot 2CH_2Cl_2$	$C_{26}H_{81}B_{20}IP_4Pt_2$
M_r	638.01	1372.96	1251.07
Colour, habit	Yellow block	Deep purple plate	Green plate
Crystal size/mm	0.50 × 0.42 × 0.40	0.40 × 0.20 × 0.05	0.20 × 0.10 × 0.05
Crystal system	Monoclinic	Triclinic	Triclinic
Space group	$P2_1/c$	$P\bar{1}$	$P\bar{1}$
a/Å	11.844(2)	9.9818(8)	10.195(1)
b/Å	13.082(1)	14.445(2)	13.582(3)
c/Å	16.385(1)	19.716(3)	18.056(2)
α/°		94.543(6)	95.97(1)
β/°	98.67(1)	96.23(1)	93.07(1)
γ/°		105.250(7)	108.43(2)
U/Å^3	2509.8(5)	2709.3(6)	2349.3(6)
Z	4	2	2
D_c/g cm^{-3}	1.688	1.683	1.769
μ(Mo-Kα)/cm^{-1}	58.30	55.03	67.64
F(000)	1240	1336	1212
2θ Range/°	4–55	4–55	4–55
Reflections measured	15 718	28 182	24 761
Unique reflections	5724	12 258	10 655
h,k,l Ranges	−15 to 15, −12 to 16, −20 to 20	−12 to 12, −18 to 18, −25 to 25	−13 to 13, −17 to 17, −23 to 23
Final residuals $wR2$ ($R1$)[a]	0.0381 (0.0159)	0.0784 (0.0344)	0.0719 (0.0330)
Weighting factors[a]	a = 0.0194, b = 0.00	a = 0.0388, b = 0.00	a = 0.0281, b = 0.00
Final electron-density difference features (maximum, minimum)/e Å^{-3}	0.89, −0.54	2.15, −2.39	2.03, −2.17
Goodness of fit on F^2	1.016	0.952	0.954

[a] $wR2 = [\Sigma w(F_o^2 - F_c^2)^2/\Sigma w(F_o^2)^2]^{\frac{1}{2}}$ where $w = [\sigma^2(F_o^2) + (aP)^2 + bP]$ and $P = [\max(F_o^2, 0) + 2F_c^2]/3$. The value in parentheses is given for comparison with refinements based on F_o with a typical threshold of $F \geqslant 4\sigma(F)$ and $R1 = \Sigma||F_o| - |F_c||/\Sigma|F_o|$, and $w^{-1} = [\sigma^2(F_o) + g|F_o|^2]$.

petroleum (2:1), this reaction produced a deep green fraction which was slowly eluted using CH_2Cl_2. This product was contaminated with [Na][*nido*-$CB_{10}H_{13}$] as evidenced from the ^{11}B-{^1H} NMR spectrum of the mixture. One equivalent of [NEt_4]I was added to a CH_2Cl_2 solution of the green compound resulting in the precipitation of a white powder. The latter was removed by filtration through a Whatman 1 μm pore size Paradisc PTFE membrane thereby yielding a sea-green solution. After concentration, layering this solution with hexane gave deep green *crystals* of [$Pt_2(PEt_3)_4$\{η^5:η$^{5'}$-9,9′-I(H)(7-$CB_{10}H_{10})_2$\}] **5** (0.15 g, 11%) (Found: C, 25.3; H, 6.5. $C_{26}H_{81}B_{20}IP_4Pt_2$ requires C, 25.0; H, 6.5%). EI mass spectrum: *m*/*z* 1251 (*M*), 1132 (*M* − PEt_3) and 1011 (*M* − 2PEt_3).

Crystallography

Crystals of compounds **3**, **4** and **5** were grown by diffusion of hexane into CH_2Cl_2 solutions. Those of **4** grow with two molecules of CH_2Cl_2 in the asymmetric unit, one of which was disordered. All crystals were mounted on glass fibres and data were collected at 173 K on a Siemens SMART CCD area-detector three-circle diffractometer (Mo-Kα X-radiation, graphite monochromator, $\bar{\lambda}$ = 0.710 73 Å). For three or four settings of φ, narrow data 'frames' were collected for 0.3° increments in ω. For the triclinic crystals (**4** and **5**) a full sphere of data was collected whilst for the monoclinic complex **3** just over a hemisphere of data was collected. It was confirmed that crystal decay had not taken place during the course of the data collections. The substantial redundancy in data allows empirical absorption corrections (SADABS)[9] to be applied using multiple measurements of equivalent reflections. The data frames were integrated using SAINT,[9] the structures solved by conventional direct methods and refined by full-matrix least squares on all F^2 data using Siemens SHELXTL, version 5.03.[9]

For all structures the non-hydrogen atoms were refined with anisotropic thermal parameters. Cage carbon atoms were identified from the magnitudes of their anisotropic thermal parameters and from a comparison of bond lengths to adjacent boron atoms. For complex **5** the hydrogen atom H(1) attached to the I was located from a final difference electron-density synthesis but its coordinates were not refined. All other hydrogen atoms were included in calculated positions and allowed to ride on the parent boron or carbon atoms with isotropic thermal parameters ($U_{iso} = 1.2U_{iso\ equiv}$ of the parent atom except for Me protons where $U_{iso} = 1.5U_{iso\ equiv}$).

The final electron-density difference syntheses for compounds **4** and **5** showed significant residual peaks in the vicinity of the transition-metal atoms and reflect the comparatively poor quality of the crystals available for data collection and an inability to correct completely for residual absorption effects. All calculations were carried out on Silicon Graphics Iris, Indigo or Indy computers and experimental data are recorded in Table 5.

CCDC reference number 186/923.

Acknowledgements

We thank Dr. Paul A. Jelliss for helpful discussions and the Robert A. Welch Foundation for support (Grant AA-1201).

References

1 S. A. Batten, J. C. Jeffery, P. L. Jones, D. F. Mullica, M. D. Rudd, E. L. Sappenfield, F. G. A. Stone and A. Wolf, *Inorg. Chem.*, 1997, **36**, 2570.
2 R. N. Grimes, in *Comprehensive Organometallic Chemistry II*, eds. E. W. Abel, F. G. A. Stone and G. Wilkinson, Pergamon, Oxford, 1995, vol. 1 (ed. C. E. Housecroft), ch. 9.
3 A. G. Orpen, L. Brammer, F. H. Allen, O. Kennard, D. G. Watson and R. Taylor, *J. Chem. Soc.*, *Dalton Trans.*, 1989, S1.
4 Z. Janousek, B. Stíbr, X. L. R. Fontaine, J. D. Kennedy and M. Thornton-Pett, *J. Chem. Soc.*, *Dalton Trans.*, 1996, 3813.
5 A. I. Yanovskii, Yu. T. Struchkov, V. V. Grushin, T. P. Tolstaya and I. I. Demkina, *Zh. Strukt. Khim.*, 1988, **29**, 89.
6 J. Plešek, T. Jelínek, E. Drdakova, S. Heřmánek and B. Stíbr, *Collect. Czech. Commun.*, 1984, **49**, 1559.
7 G. W. Parshall, *Inorg. Synth.*, 1970, **12**, 26.
8 W. H. Knoth, J. L. Little, J. R. Lawrence, F. R. Scholer and L. J. Todd, *Inorg. Synth.*, 1968, **11**, 33.
9 Bruker X-ray Instruments, Madison, WI, 1995.

Received 3rd *February* 1998; *Paper* 8/00918J